Current Opinion in Colloid & Interface Science 16 (2011) 71–79

Contents lists available at ScienceDirect

Current Opinion in Colloid & Interface Science

journal homepage: www.elsevier.com/locate/cocis

Designing colloidal suspensions for directed materials assembly

Jacinta C. Conrad [a,1], Summer R. Ferreira [b], Jun Yoshikawa [b], Robert F. Shepherd [b], Bok Y. Ahn [b], Jennifer A. Lewis [b,*]

[a] Department of Chemical and Biomolecular Engineering, University of Houston, 4800 Calhoun, Houston, TX 77204-4004, United States
[b] Materials Science and Engineering Department, University of Illinois, 1304 W. Green Street, Urbana, IL 61801, United States

ARTICLE INFO

Article history:
Received 1 June 2010
Accepted 30 October 2010
Available online 5 November 2010

ABSTRACT

Recent advances in microfluidic and direct-write assembly of colloidal suspensions open new avenues for microscale patterning of functional materials with controlled composition, geometry, and properties. In this article, we describe fundamental aspects of suspension structure, elasticity, and flow behavior for three important systems: (1) dense liquids (and glasses), (2) gels, and (3) biphasic mixtures. We also highlight examples from the current literature of colloidal architectures patterned by these emerging methods.

1. Introduction

The ability to pattern colloidal suspensions in planar and three-dimensional motifs is critical for myriad technologies, including optical displays, designer pharmaceuticals, micro-electromechanical systems, and printed electronics. The broad diversity of potentially relevant materials, length scales, and architectures underscores the need for flexible patterning approaches. Emerging routes based on microfluidic [1•,2••] and direct-write assembly [3••] enable the rapid design and fabrication of colloidal materials without the need for expensive tooling, dies, or lithographic masks, and therefore offer exciting opportunities for materials assembly.

Colloidal suspensions used in these directed assembly methods must flow without clogging through confined geometries [4], such as microchannel(s) or nozzle(s) within the fluidic device or printhead. The desired flow behavior can be achieved by carefully controlling three key parameters: the colloid volume fraction, ϕ, interparticle attraction strength, U, and applied stress, σ, as shown in Fig. 1a [5••]. These parameters also strongly influence the structure and elasticity of colloidal suspensions, which enable patterned structures to retain their shape and solidity after forming. In this article, we first describe three types of dense colloidal suspensions that can be designed for the microfluidic and direct-write assembly methods of interest: dense fluids and glasses, gels, and biphasic mixtures. Next, we introduce examples from the current literature of patterned colloidal architectures, ranging from novel granular media to flexible, stretchable, and spanning microelectrodes for printed electronics. Finally, opportunities and challenges associated with these emerging methods are highlighted.

2. Designing colloidal suspensions

2.1. Suspension structure

The design of colloidal suspensions for microfluidic and direct-write assembly requires a fundamental understanding of the relationship between suspension microstructure and properties. Three systems of interest, namely concentrated colloidal fluids and glasses, gels, and biphasic mixtures, are highlighted in Fig. 1b–d. Concentrated colloidal fluids undergo a nonequilibrium transition to a glassy state as the volume fraction, ϕ, is increased above a critical value ϕ_{glass} [6]. The suspension structure remains disordered even above the glass transition [7], as shown in Fig. 1b for hard-spheres that interact only through infinite repulsion at contact (i.e., $U=0$ for $h>0$, where h is the minimum separation distance between a pair of colloids). However, particle dynamics become arrested when $\phi>\phi_{glass}$, as individual particles become trapped in cages formed by their nearest neighbors. To avoid cage-driven jamming and solidification, microfluidic assembly routes typically use dense colloidal fluids rather than colloidal glasses [1•,2••].

Distinct non-equilibrium arrested states can be obtained in colloidal systems by introducing an attractive interparticle potential (i.e., $U>0$ over some h range). When this attraction is sufficiently strong (~ a few k_bT or higher) and the colloid volume fraction exceeds the gel point ϕ_{gel}, the colloidal particles aggregate to form a system-spanning interconnected network that is both disordered and dynamically arrested. When $\phi<0.1$, the structure of these dilute colloidal gels is well described as a network of fractal aggregates [8,9••], while at higher volume fraction the gel structure is composed of weakly interconnected, dense clusters separated by heterogeneous voids [10,11]. Concentrated colloidal gels ($\phi\sim0.5$) are of interest as "inks" for direct-write assembly. The inks are first formulated as concentrated fluids and subsequently gelled to induce the desired viscoelastic response for printing. One representative example of a colloidal ink, composed of cationic polyelectrolyte-coated silica

* Corresponding author. Tel.: +1 217 244 4973; fax: +1 217 244 2278.
E-mail address: jalewis@illinois.edu (J.A. Lewis).
[1] Tel.: +1 713 743 3829; fax: +1 713 743 4323.

1359-0294/$ – see front matter
doi:10.1016/j.cocis.2010.11.002

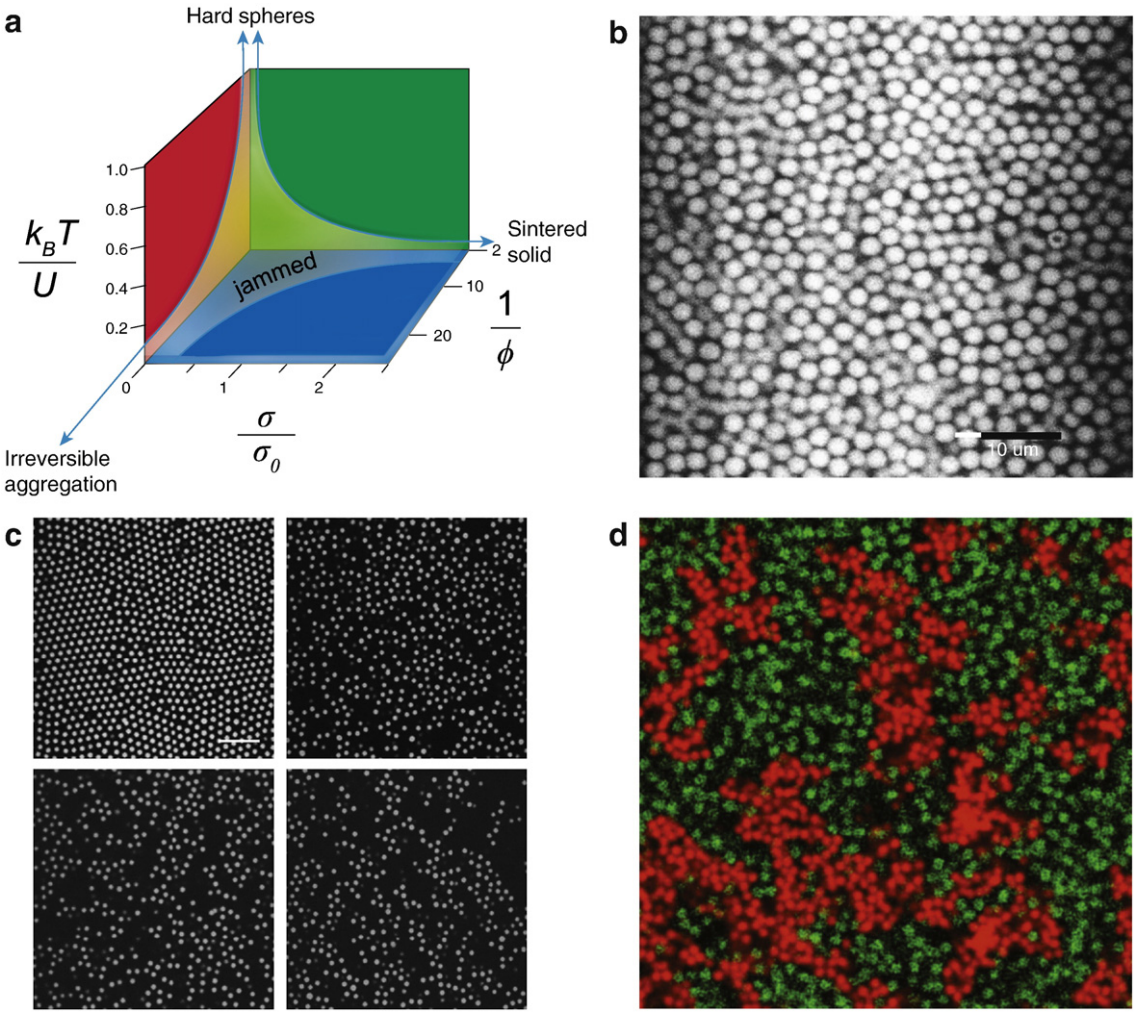

Fig. 1. (a) Jamming phase diagram for attractive colloidal particles. Reprinted by permission from Macmillan Publishers Ltd: Nature (Ref. [5••]), copyright 2001. (b) Confocal micrographs of a colloidal glass with $\phi = 0.61$. Reprinted in part with permission from reference [38]. Copyright 2007 IOP Publishing Ltd. (c) Confocal micrographs of a colloidal suspension with $\phi = 0.02$ after settling, with EDTA concentration of (top left) 0 mM; (top right) 300 mM; (bottom left) 600 mM; (bottom right) 900 mM. The scale bar is 5 μm. Reprinted in part with permission from reference [12]. Copyright 2009 American Chemical Society. (d) Confocal micrograph of a biphasic mixture with $\phi_{att} = \phi_{rep} = 0.05$ (i.e. $\phi_{tot} = 0.1$). Reprinted figure with permission from reference: A. Mohraz, E. R. Weeks, and J. A. Lewis, Phys. Rev. E 77, 060403 (2008) [18••]. Copyright 2008 by the American Physical Society.

microspheres gelled by the addition of salt, is shown in Fig. 1c [12]. In the absence of salt, the highly charged microspheres assemble into a crystalline sediment, whereas above a critical salt concentration a gel network forms. The pronounced changes in gel morphology with increasing ionic strength reflect the intensified attractive interactions between particles, which allow the ink to better support its own weight even as it spans unsupported regions.

To date, colloidal inks used for direct-write assembly have been composed of pure colloidal gels with uniform interparticle interactions, in which ϕ and U have been carefully tuned [3,13••,14–17]. However, the presence of clusters within the gel limits the minimum nozzle size through which these inks can be flowed, even when the primary particle size is relatively small. To obtain additional control over the suspension microstructure, a new type of colloidal system was recently introduced, referred to as a biphasic mixture [18••], in which the interparticle interactions of coexisting particle populations were independently tuned. One population was composed of attractive particles that aggregated to form a gel network, while the other population of particles remained stable, adhering to neither the attractive nor the repulsive species [18••]. In all other respects, the attractive and repulsive particles were identical.

Biphasic mixtures represent a new paradigm for designing colloidal suspensions that enables additional control over their structure and dynamics [18••]. These properties can be precisely tuned simply by altering the relative fractions of the two species at a fixed ϕ and U. Two types of biphasic systems have been recently introduced: one composed of partially hydrophobic and hydrophilic colloids [18••] and the other composed of polyelectrolyte- and comb polymer-coated colloids [12], both of which are suspended in an aqueous-based solution. In the first system, the hydrophilic particles are repulsive, while the partially hydrophobic particles are attractive (Fig. 1d). In the second system, charge-neutral teeth along the comb polymer backbone enable this population to remain stable over a broad range of pH, ionic strength, and flocculant concentrations, whereas the polyelectrolyte-coated particles undergo gelation when the solution conditions are altered. Direct imaging of biphasic mixtures revealed that each particle population exhibits distinct dynamical properties: the repulsive population exhibits the diffusive dynamics of a colloidal fluid, whereas the attractive population exhibits the arrested dynamics expected of a colloidal gel. Furthermore, the presence of the repulsive species modifies the structure of the aggregated network: as the concentration of repulsive particles is increased, attractive particles have fewer attractive neighbors, leading to a more spatially homogeneous network [18••]. These observations have important consequences for the elasticity and yielding behavior of biphasic mixtures, which differ considerably from pure colloidal gels.

2.2. Elasticity and yielding

Colloidal suspensions developed for microfluidic and direct-write assembly methods must flow readily through microchannels and fine deposition nozzles, respectively. Microfluidic assembly methods require dense colloidal fluids that exhibit shear thinning behavior and a negligible shear yield stress τ_y [1•,2••]. By contrast, direct-write assembly requires concentrated colloidal inks that must first yield and flow when extruded through a fine deposition nozzle, yet quickly recover an elastic-like response upon exiting the nozzle so that the ink can support its own weight in spanning architectures. Colloidal inks designed for direct-write assembly must therefore possess both a finite τ_y and a zero-shear-rate elastic modulus G' [13••,14]. Colloidal gels and biphasic mixtures are excellent candidates given that they exhibit the desired rheological behavior.

For dense colloidal fluids ($\phi<\phi_{glass}$), the viscous modulus G'' is greater than the elastic modulus G′ and both scale approximately as power laws with frequency, G''~ω^2 and G′~ω. As ϕ is increased above ϕ_{glass}, these suspensions undergo a fluid-to-solid transition that is signaled by the appearance of a finite yield stress τ_y; these suspensions yield and flow when the applied shear stress exceeds τ_y. Concomitantly, the linear viscoelastic response of these systems becomes increasingly dominated by G′ [19••]. Microscopically, the elasticity of colloidal glasses results from the presence of topological cages that resist deformation, and yielding occurs when these cages are disrupted [20,21]. In the glassy state, both τ_y and G′ depend sensitively upon ϕ, scaling as a power law with typical exponents ranging from 9 to 15 (Fig. 2a) [22]. The observed ϕ dependence is in good agreement with that predicted by a microscopic statistical mechanical theory, based on a nonequilibrium free energy, which incorporates both local cage correlations and activated barrier hopping processes [23•, 24]. However, the predicted values of G′ and τ_y are over an order of magnitude greater than the experimental values for these nanoparticle glasses. This quantitative difference between theory and experiment may result from the "soft" repulsive interaction between nanoparticles that arises due to the presence of a polyelectrolyte adlayer; further research is needed to fully elucidate adlayer effects on mechanical properties. The strong dependence of G′ on ϕ is deleterious for direct-write assembly, since small fluctuations in the local composition can induce large changes in the mechanical properties, giving rise to clogging in constrained geometries.

Colloidal gels are viscoelastic materials that exhibit finite values of the low-shear elasticity and yield stress. For these systems, G′ and τ_y can be increased by either increasing ϕ or reducing the volume fraction ϕ_{gel} at which the fluid-to-gel transition occurs. Both G′ and τ_y exhibit a power law dependence on ϕ; however, the scaling exponents, which range from 3 to 5, are significantly smaller than those seen for colloidal glasses [25]. For example, G′ and τ_y (not shown) scale as $\phi^{3.6}$ in colloidal gels composed of partially hydrophobic silica microspheres suspended in water (Fig. 2b) [26]. The elastic moduli of gels are comparable to or greater in magnitude than those of colloidal glasses even when the volume fractions of gels are significantly smaller, due to the contribution from attractive interparticle bonds. In contrast to glasses, yielding in gels occurs when interparticle bonds are disrupted under high applied stresses ($\tau>\tau_y$); the yield strains measured for colloidal gels are thus typically smaller than those measured for colloidal glasses [21]. The presence of attractive bonds between particles also enhances the gel's resistance to local consolidation relative to that of a colloidal glass. Colloidal gel-based inks used for direct-write assembly typically employ high ϕ~0.5 to minimize drying shrinkage after printing [13••,15]. Hence, the primary control parameter is the strength of the attraction between particles, U, which strongly influences ϕ_{gel} [5••]. Based on recent experiments and simulations on model depletion gels [27–30], we estimate that a minimum interparticle attraction of order $O(10)$ k_BT is required to achieve the mechanical solidity needed to produce space-spanning structures via direct-write assembly.

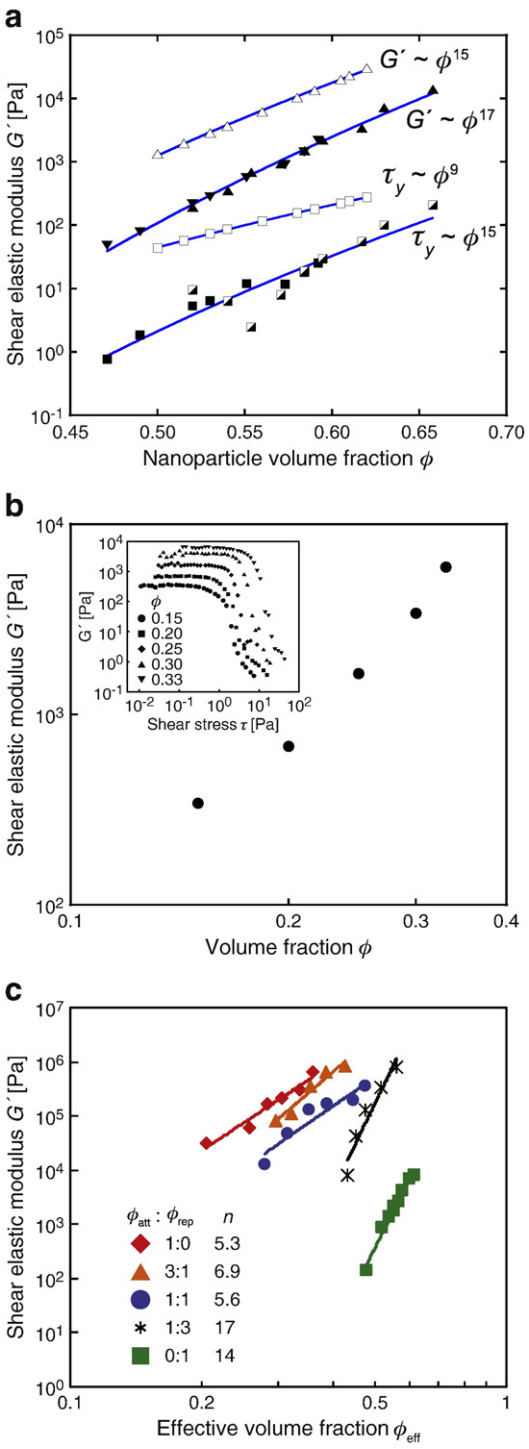

Fig. 2. (a) Shear elastic modulus (G', triangles), and shear yield stress (τ_y, squares) as a function of nanoparticle effective volume fraction ϕ, comparing experimental data (filled symbols) to theoretical predictions (open symbols). Reprinted in part with permission from reference [22]. Copyright 2006 American Chemical Society. (b) Shear elastic modulus G' as a function of colloid volume fraction ϕ. Inset: shear elastic modulus G' versus shear stress τ. Reprinted in part with permission from [26]. Copyright 2007 American Chemical Society. (c) Shear elastic modulus G' as a function of nanoparticles effective volume fraction ϕ for mixtures composed of attractive and repulsive particles.

Biphasic mixtures composed of attractive and repulsive colloids exhibit structural and dynamical features characteristic of both gels and glasses [18••]. At fixed ϕ and U, the ratio between the attractive and repulsive particle volume fractions (ϕ_{att}:ϕ_{rep}, where $\phi=\phi_{att}+\phi_{rep}$) provides an additional mechanism parameter by which to control the

elasticity and yielding behavior of these suspensions. Recent measurements carried out on biphasic mixtures composed of polyelectrolyte- (attractive) and comb polymer-coated (repulsive) nanoparticles are shown in Fig. 2c. For suspensions composed solely of repulsive particles ($\phi_{att}:\phi_{rep}=0:1$), the low-shear-rate elastic modulus increases with volume fraction as $G' \sim \phi^{14}$, consistent with the scaling exponents of a colloidal glass. Upon adding a small fraction of attractive particles to increase the ratio to $\phi_{att}:\phi_{rep}=1:3$, G' increases substantially at comparable effective volume fractions, indicating that interparticle bonds contribute to suspension elasticity; nonetheless, the scaling exponent $G' \sim \phi^{17}$ is still typical of a colloidal glass. However, at an even higher attractive particle ratio of $\phi_{att}:\phi_{rep}=1:1$, the scaling behavior abruptly changes to $G' \sim \phi^{5.6}$, consistent with that observed for colloidal gels. Indeed, recent theoretical work confirms that their phase behavior and dynamics depend in a complicated fashion upon $\phi_{att}:\phi_{rep}$, ϕ and U [31•]. Because biphasic mixtures combine the resistance to consolidation of colloidal gels with the high solids loading of glasses, they may offer important advantages for printing colloidal architectures through microscale nozzles. These nascent observations underscore the need for additional routes for generating biphasic mixtures as well as fundamental studies of their structure, dynamics, rheology, and printing behavior.

2.3. Flow behavior in uniform and constricted microchannels

Relating the structure of dense colloidal suspensions to their flow behavior through uniform [32,33•,34,35•] and constricted microchannels [36] is of paramount importance for microfluidic and direct-write assembly. Both methods require flow of concentrated suspensions through microchannels or deposition nozzles whose characteristic size ranges from 1 to 250 μm [37]. Effects due to confinement in channels, such as wall slip and transient clogging, may promote further restructuring beyond that induced by hydrodynamic forces [36] or hetero-coagulation [4] during flow. Elucidating the complex interplay between confinement, structure, and flow behavior for concentrated colloidal suspensions is therefore crucial for fully exploiting these emerging fabrication methods.

One technique that allows direct interrogation of structure in three dimensions during flow is confocal microscopy [38]. This technique has been successfully used to investigate the structure of quiescent colloidal glasses [39], gels [9,40,41], and biphasic mixtures [18••]. Standard particle-tracking algorithms allow the positions of micron-sized particles to be followed over many hours in quiescent suspensions [42••]; however, obtaining quantitative information about colloidal structure and trajectories as they undergo flow through confined geometries presents additional challenges. Particle-tracking algorithms require that particles move less than the interparticle spacing between consecutive frames; however, the flow velocities of micron-sized particles in microchannels can easily exceed 100 μm/s. Single particles may move more than a particle diameter between frames even when the acquisition rate is as high as 100–200 frames/s, clearly hindering particle tracking. To obtain quantitative information on particle positions and velocities during flow, particle motions are instead analyzed in a co-moving reference frame in which relative displacements are small [35•]. Briefly, the displacement for co-moving regions of an image (rectangles for one-dimensional motion [33•], squares for two-dimensional motion [43]) is calculated by maximizing the cross-correlation between corresponding regions in consecutive images in a time series taken during flow. This displacement is subtracted from the particle positions, and particles are then tracked normally in the co-moving reference frame using the existing algorithms. To recover the trajectories in the original stationary reference frame, the displacement is then added back to the particle positions after tracking [35•].

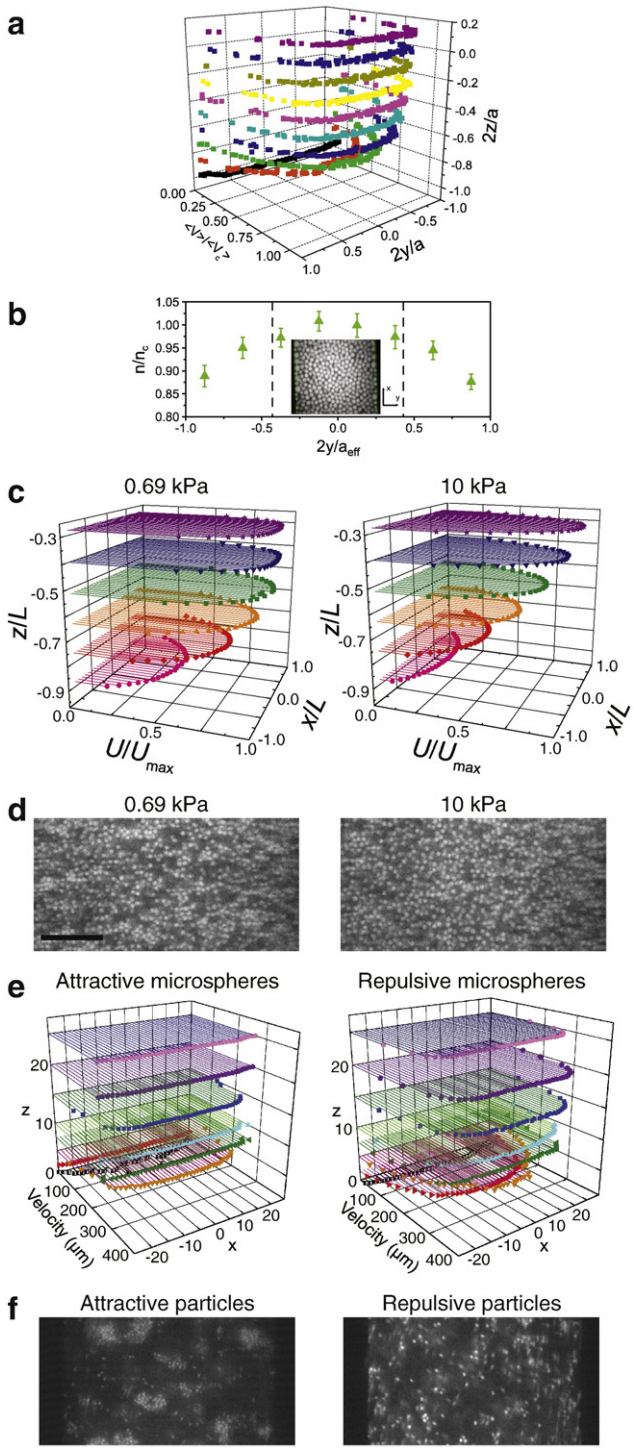

Fig. 3. (a) Normalized velocity profiles of a colloidal glass with $\phi \geq 0.63$ as a function of height, in a square microchannel with inner diameter 50 μm. (b) Normalized density profile n/n_c as a function of normalized lateral position y/a_{eff} in the microchannel, where a_{eff} is the effective channel diameter for a microchannel with rough walls, for a height $z=17$ μm. Reprinted figures in (a) and (b) with permission from: L. Isa, R. Besseling, and W. C. K. Poon, Phys. Rev. Lett. 98, 198305 (2007) [33•]. Copyright 2007 by the American Physical Society. (c) Normalized flow profiles of a colloidal gel with $\phi=0.27$ in a square microchannel with inner diameter 50 μm, at applied pressures of (left) 0.69 kPa and (right) 10 kPa. (d) Confocal micrographs of a colloidal gel with $\phi=0.27$ flowing under an applied pressure of (left) 0.69 kPa and (right) 10 kPa taken 3 μm above the bottom surface of the microchannel. The scale bar is 10 μm. (c) and (d) reprinted with permission from reference [46•]. Copyright 2008 American Chemical Society. (e) Normalized flow profiles of the (left) attractive and (right) repulsive particles in a biphasic mixture with $\phi=0.35$ and $\phi_{att}:\phi_{rep}=3:1$ flowing in a square microchannel with inner diameter 50 μm at a volumetric flow rate of 41 nL/min. (f) Confocal micrographs of a biphasic colloidal mixture with $\phi=0.35$ and $\phi_{att}:\phi_{rep}=3:1$ flowing in a square microchannel with inner diameter 50 μm at a volumetric flow rate of 50 nL/min, taken 5 μm above the bottom surface of the microchannel.

The combination of confocal microscopy and flow-based tracking algorithms is a central feature of recent investigations that correlate microstructure with the flow behavior of concentrated suspensions, i.e. colloidal fluids [44,45], glasses [33,34], gels [43,46•,47], and biphasic mixtures, through uniform and constricted microchannels. For yield-stress fluids, the qualitative flow behavior is determined by the ratio of yield stress to viscous stress as parameterized by the Oldroyd number $Od = \tau_y/\tau_v$, which predicts a transition from plug-like flow to fluid-like flow with full yielding at $Od \sim 0.5 - 1$. Surprisingly, colloidal glasses can exhibit plug-like flow in microchannels even at low values of $Od = 0.02$ (Fig. 3a) [33•]. The presence of transverse velocity fluctuations suggests that interparticle friction between the sterically stabilized particles influences their flow behavior, similar to dry granular materials. Indeed, flowing glassy suspensions exhibit other characteristics typical of granular media, such as variations in density across the microchannel (Fig. 3b) [33•]. Models of granular flow quantitatively describe this behavior, confirming that interparticle friction reduces the number of cage-breaking events that contribute to yielding.

For colloidal gels, yielding occurs initially when the weakest bonds between particles or clusters are broken [27,28]; thus, frictional effects may be less significant. Indeed, pressure-driven microchannel flows of colloidal gels exhibit the qualitative behavior predicted by the Oldroyd number, as shown in recent experiments on poly(ethyeleneimine)-coated silica microspheres flocculated by adding oppositely-charged poly(acrylic acid) [46•]. As the applied pressure driving flow increases, the flow profiles exhibit a transition from plug-like to fluid-like flow at $Od \sim 1$ (Fig. 3c), showing that yielding of the gel structure occurs when the viscous stress is sufficiently large. Confocal images taken during flow reveal two distinct yielding mechanisms, in agreement with quiescent results. First, when the applied pressure is small, yielding occurs predominantly between clusters. As the applied pressure increases, the clusters themselves undergo yielding as the bonds between particles are disrupted (Fig. 3d). A similar transition from plug-like to fluid-like flow in microchannels with increasing flow rate is also seen for colloidal gels flocculated via hydrophobic interactions [26]. Despite these qualitative similarities in flow behavior, different quantitative models best describe the flow profiles in each system, indicating that the details of microscopic interactions strongly affect the flow behavior.

The influence of microscopic interactions on flow behavior is further confirmed in the flow profiles measured for biphasic mixtures. For a biphasic mixture in which $\phi_{att}:\phi_{rep} = 3:1$ ($\phi = 0.35$) the attractive and repulsive microspheres exhibit qualitatively different normalized flow profiles (Fig. 3e). The velocity profiles of the attractive microspheres exhibit plug-like flow across the entire microchannel, except immediately adjacent to the microchannel walls ($z = 1$ μm). By contrast, the velocity profiles of repulsive microspheres are plug-like in the center of the channel and decrease near the walls. Direct comparison of the velocity profiles for the two species reveals that the flow of repulsive microspheres is significantly hindered compared to that of the attractive microspheres near the walls. The distribution of the two particle populations also differs across the microchannel (Fig. 3f): clusters of attractive particles are typically found nearer the vertical midplane of the channel due to excluded volume effects, whereas distinct repulsive particles are more uniformly distributed at different heights. Based on these observations, it is likely that the repulsive particles help lubricate the flow of the attractive particles through fine geometries, thereby enabling the ability to print smaller features (~10 μm) with biphasic inks than can be achieved with colloidal gels with uniform interactions (~100 μm) [15].

The influence of microchannel geometry on the flow profile is especially relevant for both microfluidic and direct-write assembly methods. In these methods, the microchannel or nozzle diameter may taper at a characteristic angle α or change abruptly ($\alpha = 90°$). Only recently, studies have begun to investigate the influence of constriction geometry on suspension structure and flow for systems relevant for directed materials assembly. For example, observations of colloidal glasses flowing into a constriction revealed that they experience repeated cycles of transient jamming [48••]: flow first slowed and locally rarefied shocks formed, as indicated by the dark arches in the two rightmost images in Fig. 4a; the static structure eventually fractured and flow increased. Similar oscillations in flow velocity are observed for colloidal glasses flowing in straight microchannels; when the width of the microchannel is sufficiently small, the flow exhibits a near-complete arrest [34]. Trajectories of particles at the transition between shear and plug flow reveal self-organized convergent flow of particles into a narrow region (Fig. 4b). These constriction-induced jamming events in glasses, whether from external or self-organized geometric constraints, are attributed to the complex interplay between shear thickening, which induces the formation of locally dense regions via jamming, and permeation flow, which erodes them [34].

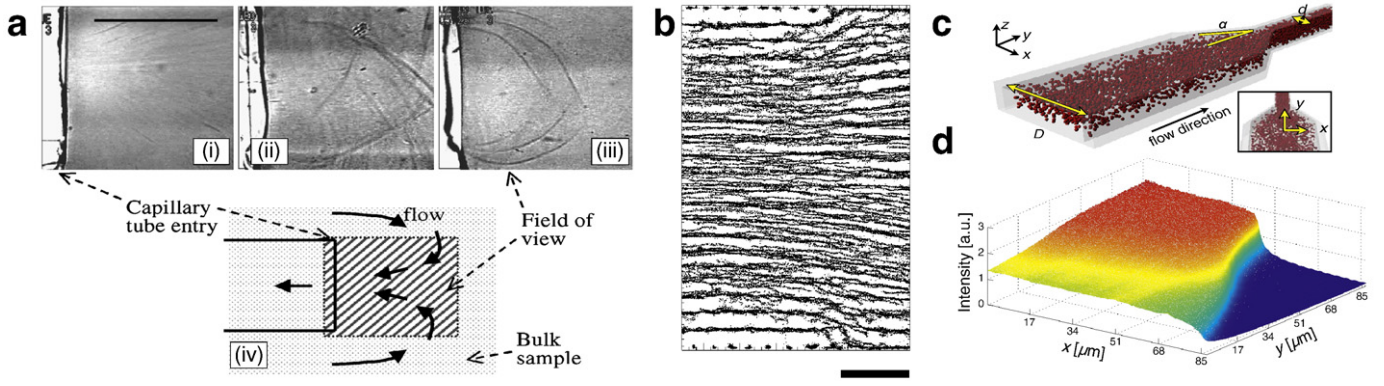

Fig. 4. (a) Images of the flow of a suspension of 1 μm colloids at volume fractions of (left) $\phi = 0.534$, (middle) $\phi = 0.578$, and (right) $\phi = 0.60$, showing the formation of arch-like "shock" regions of reduced colloid density when ϕ is sufficiently high. The horizontal line is 0.5 mm. At the left of each image the capillary entrance can be seen, as indicated by the schematic. Reprinted figure with permission from reference: M. D. Haw, Phys. Rev. Lett. 92, 185506 (2004) [48••]. Copyright 2004 by the American Physical Society. (b) Superposition of particle positions in a colloidal glass with $\phi \geq 0.63$ flowing in a square microchannel with inner diameter 50 μm, showing converging streamlines at the interface between plug flow and shear flow. Reprinted figure with permission from reference: L. Isa, R. Besseling, A. N. Morozov, and W. C. K. Poon, Phys Rev. Lett. 102, 058302 (2009) [34]. Copyright 2009 by the American Physical Society. (c) Schematic illustration of constricted microchannel flow experiments. (d) Three-dimensional representation of the intensity profile (in arbitrary units) for a gel with $\phi = 0.26$ flowing under an applied pressure of 0.7 kPa through a microchannel with $D = 150$ μm, $d = 50$ μm, and $\alpha = 27°$, at a height of 9 μm above the bottom surface of the channel, showing the increase in local density induced by the constriction. The origin used in this image is the same as that shown in (c). (c) and (d) reprinted with permission from reference [43]. Copyright 2010 American Chemical Society.

Microchannel geometry can also influence the suspension structure and flow behavior of colloidal gels. Recent observations of polyelectrolyte-bridged colloidal gels flowing through microchannel constrictions, of relevance to direct-write assembly, are shown in Fig. 4c [43]. The increase in average density of the structure downstream from the constriction (Fig. 4d) is greater than predicted for shear-enhanced migration of particles and clusters [45,49], indicating that filter pressing (i.e., preferential flow of fluid versus solid) leads to consolidation. The local structure of the gel, as quantified by Voronoi volume and coordination number [50], is not strongly affected by flow through constriction, whereas the long-length scale structure of the gel becomes more heterogeneous as the relatively weak bonds between clusters rupture. Despite differences in aggregation mechanism, the qualitative mechanisms of yielding observed for these polyelectrolyte-bridged systems are similar to those seen in depletion gels [27,28]. Their yielding behavior is advantageous for printing, since the disruption of the aggregated network into smaller clusters facilitates flow through fine geometries. Notably, the influence of constrictions on suspension structure and resulting flow profiles has yet to be investigated for biphasic colloidal mixtures. This open area of research demands attention.

The above examples demonstrate that the colloid volume fraction and interparticle interactions strongly influence the elasticity, yielding and flow behavior required for microfluidic and direct-write assembly. To further tailor the behavior of both polymer-stabilized and polymer-bridged systems used for assembly, careful studies investigating the correlation between structural and mechanical properties are needed. In addition, the resistance of a suspension to consolidation or filter pressing depends not only on its behavior under shear flow, as discussed here, but also on its compressive rheological properties [51]. Relatively little attention has been given to the latter topic for colloidal systems of interest for the directed assembly methods described below.

3. Microfluidic assembly

The assembly of colloidal architectures of controlled size, shape, and composition is central to fundamental studies of granular materials as well as to numerous applications, including sensors, optical devices, and microelectromechanical systems (MEMS). Traditional methods for producing colloidal granules, such as fluid bed granulation, high shear mixer granulation, and spray drying, do not provide adequate control over these key parameters. Other methods, such as electroplating and molding (LIGA) [52,53], micro-injection molding [54,55], micro-stereolithography [56,57], and micro-electro-discharge machining [58], lack either the materials flexibility or rapid assembly times desired for these applications. Hence, there is tremendous interest in developing new patterning methods for creating precisely tailored colloidal granules and microcomponents.

Microfluidic assembly methods have attracted considerable attention based on the discovery that monodisperse emulsion drops can be produced by co-flowing immiscible fluids within microchannels [59•, 60••, 61–63]. In early efforts, hydrogel [64,65] and polymeric particles [66–69] (ca. 10–200 μm in diameter) were produced by *in-situ* photopolymerization of monomeric drops in the form of either homogeneous [64–69] or Janus spheres [70–73] or discoids [66–69]. Recently, microfluidic devices have been used to produce colloid-filled hydrogel granules and microcomponents of tunable size, geometry, and composition [1•,2••].

In one example, a microfluidic sheath-flow device was used to assemble monodisperse colloid-hydrogel granules (Fig. 5a) [1•]. A dense

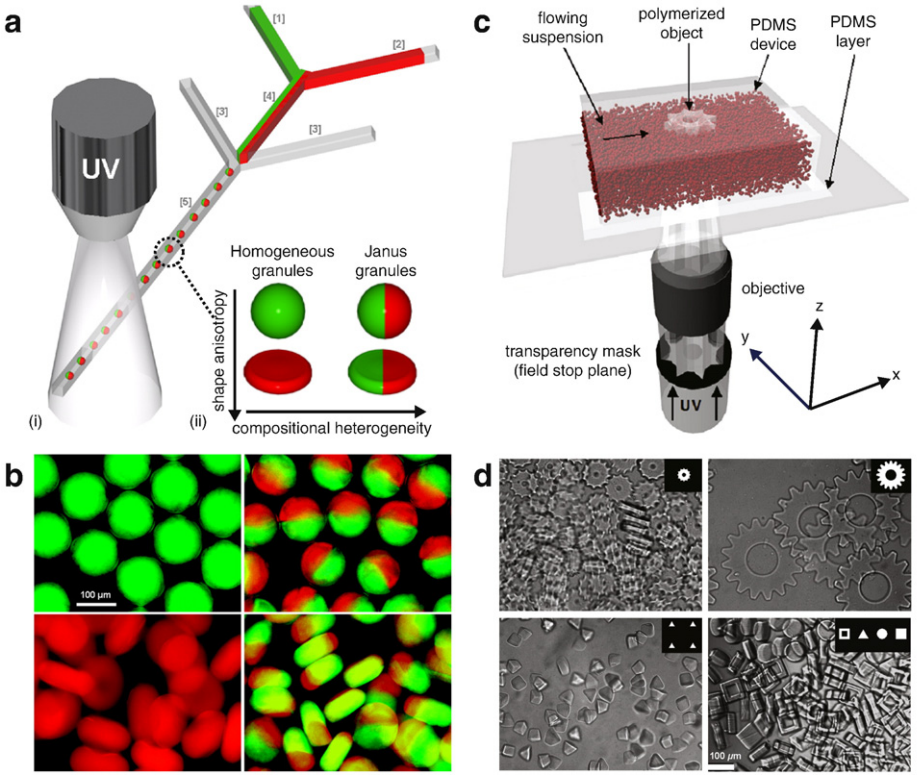

Fig. 5. (a) Schematic of the sheath-flow device used for microfluidic assembly of colloidal granules, with a schematic showing shapes and compositions explored. (b) Fluorescence images of spherical (top row) or discoidal (bottom row) and chemically homogeneous (left column) or Janus (right column) granules formed via microfluidic assembly. (a) and (b) reprinted in part with permission from reference [1•]. Copyright 2006 American Chemical Society. (c) Schematic for stop-flow lithography (SFL) of colloidal microcomponents, where a photocurable index-matched colloidal suspension is flowed through a PDMS microchannel, brought to a complete stop, photopolymerized by exposure to UV light through a mask, and ejected from the region via re-initiation of flow. (d) Optical images of microcomponents formed via SFL; scale bar is 100 μm. (c) and (d) copyright Wiley-VCH Verlag GmbH & Co. KGaA. Reproduced with permission (Ref. [2••]).

colloidal suspension (ϕ~0.35) containing a photocurable acrylamide solution was formulated, and flow focusing [61] was used to drive its breakup into colloid-filled emulsion drops. Upon exposing the drops to UV light downstream within the microchannel, they solidified into colloidal granules of the desired shape, size, and composition. The polymerized hydrogel immobilizes the colloidal species, thereby preserving the granule structure even as it exits the device. Both spherical and discoidal granules were produced in homogeneous and Janus motifs by varying the microchannel geometry and composition of the coflowing immiscible liquids, respectively, as shown in Fig. 5b [1•]. However, due to surface tension, only spherical shapes or deformations thereof can be produced in drop-generating devices, which is a major limitation of this approach.

Stop-flow lithography (SFL) [74••] represents an alternate approach that enables a rich array of simple and complex shapes to be produced, in parallel, at production rates in excess of 10^3 min^{-1}. SFL employs microscope projection photolithography [75••] to create patterned structures within a microfluidic device, eliminating the need for expensive masks or clean room conditions. In initial demonstrations, SFL was used to create polymeric particles for biomolecular analysis [76] and Janus particles [77,78]. Recently, this approach was adopted to pattern non-spherical colloidal granules and microcomponents [2••]. An index-matched colloid-filled hydrogel suspension ($\phi = 0.5$) was designed that could be flowed through a uniform microchannel and rapidly photopolymerized within the SFL device. During patterning, the suspension was stopped, exposed to UV light and photopolymerized, and then flowed again (Fig. 5c). Using different mask designs, colloidal granules and microcomponents were assembled in microgear, triangular, discoid, cuboid, and rectangular shapes (Fig. 5d). Fundamental studies of the packing behavior of these novel granular media are underway. Additionally, facile pathways were demonstrated by which these colloidal architectures could be transformed into both porous and dense oxide (silica glass) and non-oxide (silicon) structures that may find potential use in low-cost MEMS devices [2••]. The extension of this technique to a broader array of suspension compositions, including non-index matched systems, should be explored.

4. Direct-write assembly

The term "direct-write assembly" broadly describes fabrication methods that employ a computer-controlled translation stage to move a pattern-generating device, such as an ink deposition nozzle, to create materials with controlled architecture and composition. Colloidal materials in planar and three-dimensional motifs have been patterned by droplet and filamentary methods for applications that include printed electronics, photonics, advanced ceramics, sensors, composites, and tissue engineering scaffolds [3•,79,80]. Traditional methods for producing colloidal components, such as screen printing, extrusion, slip casting and injection molding, are often limited by either the minimum dimensions or geometric complexity required. Many targeted applications require microscale planar features or 3D periodic lattices, neither of which can be fabricated by traditional methods or droplet-based techniques such as inkjet printing. Hence, there is significant interest in developing colloidal inks for filamentary patterning of precisely tailored colloidal architectures.

In one striking example, omnidirectional printing of silver nanoparticle inks was introduced to create flexible, stretchable, and spanning microelectrodes for printed electronics [3••,81,82] (Fig. 6a). Concentrated, viscoelastic nanoparticle inks (>70 wt.% solids, $G' \geq 2000$ Pa) were synthesized that readily flowed through fine deposition nozzles (diameter = 1–30 mm), spanned large gaps (~1 cm) and exhibited low electrical resistivity ($\rho \sim 10^{-5}\ \Omega$cm) upon annealing at modest temperatures ($T \geq 250$ °C). Using this approach, 1D periodic (not shown) and interdigitated microelectrode arrays (Fig. 6b) were patterned through 1 μm, 5 μm, 10 μm and 30 μm cylindrical nozzles. In a single pass, printed features with aspect ratios (h/w) of ~0.7 were obtained with a minimum width of ~2 μm, which is more than an order of magnitude narrower than those produced by screen-printing [81] or inkjet printing [82].

Using omnidirectional printing, silver microelectrodes composed of stretchable, wavy, arched, and spanning features were also patterned. As one example, stretchable silver arches were printed by spanning a silver microelectrode across a pre-strained spring (inset to Fig. 6c), which was then released to form the desired arches and

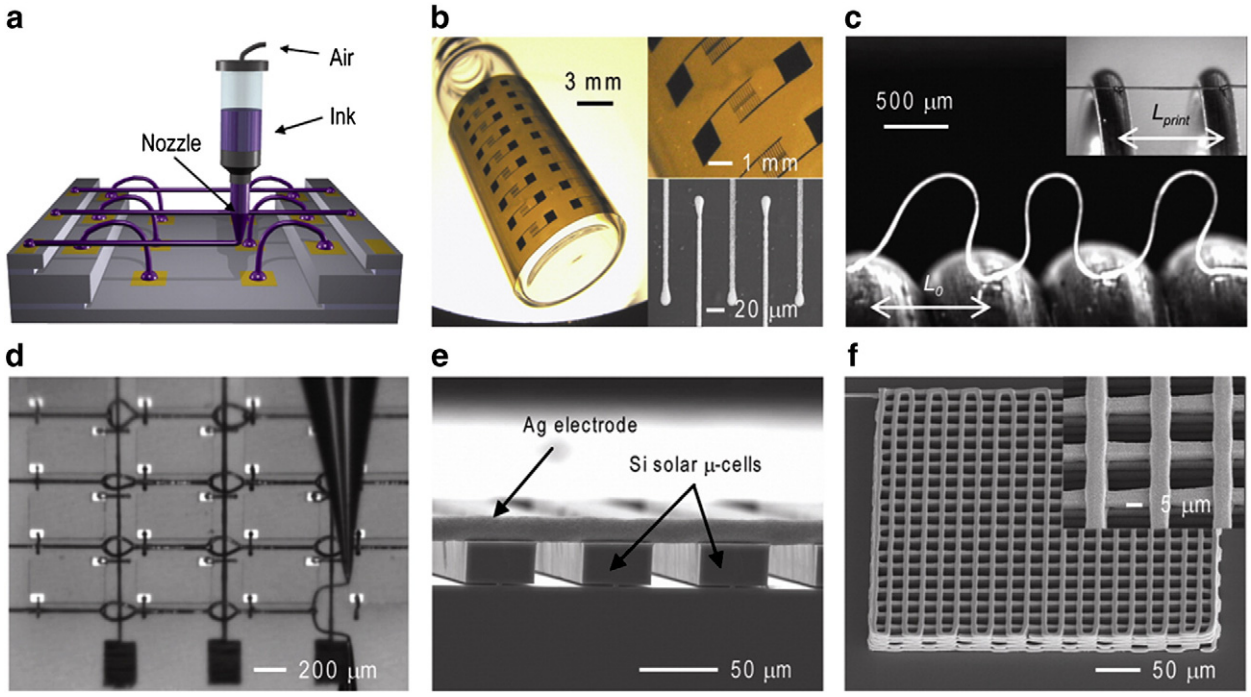

Fig. 6. (a) Schematic of omnidirectional printing of silver nanoparticle inks. (b) Optical and SEM images of silver microelectrodes patterned on a polyimide substrate with a bend radius of 14 mm. (c) Optical image of stretchable silver arches printed onto a spring. (d) Optical image acquired during patterning of silver interconnects on a gallium arsenide-based, 4×4 LED chip array. (e) Optical image of a spanning silver microelectrode printed onto an unplanarized, silicon solar microcell array. (f) SEM image of 3D periodic silver lattice. (a)–(e) adapted from reference [3••]. Copyright 2009 AAAS.

annealed (Fig. 6c). When combined with other processes such as transfer printing, direct-write assembly enables the heterogeneous integration of dissimilar materials [83,84]. To highlight these capabilities, silver microelectrodes were patterned to intercconnect both the light emitting diode (LED) and solar microcell arrays shown in Fig. 6d–e, respectively. Additionally, these viscoelastic inks could also be patterned in the form of 3D microperiodic lattices (Fig. 6f). While this method offers a powerful route for patterning microscale features, efforts are needed to improve the relatively modest printing speeds demonstrated to date.

5. Conclusions

Recent progress in the fundamental understanding and application of dense colloidal fluids, gels, and biphasic mixtures is opening new avenues for directed materials assembly. By tailoring suspension structure, dynamics, and rheology, colloidal systems have been designed for microfluidic and direct-write assembly methods. These patterning techniques provide greatly enhanced control over composition and architecture, which is required for applications ranging from novel granular media to printed electronics. Multiple advances are necessary to transform these methods into large-scale manufacturing platforms, including the design of suspensions for high-speed assembly, strategies to efficiently mix dense colloidal systems in confined geometries, and the design of 3D microfluidic devices and micronozzle arrays for parallel, scalable assembly. Together, these innovations will drive the next generation of colloidal architectures for structural, functional, and biological applications.

Acknowledgments

The authors gratefully acknowledge support from the U.S. Department of Energy, Division of Materials Science and Engineering under Award Nos. DEFG-02-07ER46472 and DOE-SC0001293 and the U.S. National Science Foundation under Grants DMR-0652424, DMR-0642573, and CMMI 07-49028.

References and recommended readings[•,••]

[1] Shepherd RF, Conrad JC, Rhodes SK, Link DR, Marquez M, Weitz DA, et al. Microfluidic assembly of homogeneous and Janus colloid-filled hydrogel granules. Langmuir 2006;22:8618–22.
[2] Shepherd RF, Panda P, Bao Z, Sandhage KH, Hatton TA, Lewis JA, et al. Stop-flow lithography of colloidal, glass, and silicon microcomponents. Adv Mater 2008;20:4734–9.
[3] Ahn BY, Duoss EB, Motala MJ, Guo X, Park S-I, Xiong Y, et al. Omnidirectional printing of flexible, stretchable, and spanning silver microelectrodes. Science 2009;323:1590–3.
[4] Georgieva K, Dijkstra DJ, Fricke H, Willenbacher N. Clogging of microchannels by nano-particles due to hetero-coagulation in elongational flow. J Colloid Interface Sci 2010;352:265–77.
[5] Trappe V, Prasad V, Cipelletti L, Segrè PN, Weitz DA. Jamming phase diagram for attractive particles. Nature 2001;411:772–5.
[6] Pusey PN. Colloidal glasses. J Phys Condens Matter 2008;20:494202.
[7] Tanaka H, Kawasaki T, Shintani H, Watanabe K. Critical-like behaviour of glass-forming liquids. Nat Mater 2010;9:324–31.
[8] de Rooij R, van den Ende D, Duits MHG, Mellema J. Elasticity of weakly aggregating polystyrene latex dispersions. Phys Rev E 1994;49:3038–49.
[9] Dinsmore AD, Prasad V, Wong IY, Weitz DA. Microscopic structure and elasticity of weakly aggregated colloidal gels. Phys Rev Lett 2006;96:185502.
[10] Ramakrishnan S, Gopalakrishnan V, Zukoski CF. Clustering and mechanics in dense depletion and thermal gels. Langmuir 2005;21:9917–25.
[11] Segrè PN, Prasad V, Schofield AB, Weitz DA. Glasslike kinetic arrest at the colloidal-gelation transition. Phys Rev Lett 2001;86:6042–5.
[12] Rhodes SK, Lambeth RH, Gonzales J, Moore JS, Lewis JA. Cationic comb polymer superdispersants for colloidal silica suspensions. Langmuir 2009;25:6787–92.
[13] Smay JE, Cesarano J, Lewis JA. Colloidal inks for directed assembly of 3-D periodic structures. Langmuir 2002;18:5429–37.
[14] Smay JE, Gratson GM, Shepherd RF, Cesarano J, Lewis JA. Directed colloidal assembly of 3D periodic structures. Adv Mater 2002;14:1279–83.
[15] Li Q, Lewis JA. Nanoparticle inks for directed assembly of three-dimensional periodic structures. Adv Mater 2003;15:1639–43.
[16] Rao RB, Krafcik KL, Morales AM, Lewis JA. Microfabricated deposition nozzles for direct-write assembly of three-dimensional periodic structures. Adv Mater 2005;17:289–93.
[17] Ahn BY, Shoji D, Hansen CJ, Hong E, Dunand DC, Lewis JA. Printed origami structures. Adv Mater 2010;22:2251–4.
[18] Mohraz A, Weeks ER, Lewis JA. Structure and dynamics of biphasic colloidal mixtures. Phys Rev E 2008;77:060403(R).
[19] Mason TG, Weitz DA. Linear viscoelasticity of colloidal hard-sphere suspensions near the glass transition. Phys Rev Lett 1995;75:2770–3.
[20] Petekidis G, Vlassopoulos D, Pusey PN. Yielding and flow of colloidal glasses. Faraday Discuss 2003;123:287–302.
[21] Pham KN, Petekidis G, Vlassopoulos D, Egelhaaf SU, Poon WCK, Pusey PN. Yielding behavior of repulsion- and attraction-dominated colloidal glasses. J Rheol 2008;52:649–76.
[22] Rao RB, Kobelev VL, Li Q, Lewis JA, Schweizer KS. Nonlinear elasticity and yielding of nanoparticle glasses. Langmuir 2006;22:2441–3.
[23] Kobelev VL, Schweizer KS. Strain softening, yielding, and shear thinning in glassy colloidal suspensions. Phys Rev E 2005;71:021401.
[24] Kobelev VL, Schweizer KS. Nonlinear elasticity and yielding of depletion gels. J Chem Phys 2005;123:164902.
[25] Buscall R, Mills PDA, Goodwin JW, Lawson DW. Scaling behavior of the rheology of aggregate networks formed from colloidal particles. J Chem Soc Faraday Trans I 1988;84:4249–60.
[26] Roberts MT, Mohraz A, Christensen KT, Lewis JA. Direct flow visualization of colloidal gels in microfluidic channels. Langmuir 2007;23:8726–31.
[27] Conrad JC, Wyss HM, Trappe V, Manley S, Miyazaki K, Kaufman LJ, et al. Arrested fluid–fluid phase separation in depletion systems: implications of the characteristic length on gel formation and rheology. J Rheol 2010;54:421–38.
[28] Laurati M, Petekidis G, Koumakis N, Cardinaux F, Schofield AB, Brader JM, et al. Structure, dynamics, and rheology of colloid–polymer mixtures: from liquids to gels. J Chem Phys 2009;130:134907.
[29] Lee MH, Furst EM. Response of a colloidal gel to a microscopic oscillatory strain. Phys Rev E 2008;77:041408.
[30] Lois G, Blawzdziewicz J, O'Hern CS. Jamming transition and new percolation universality classes in particulate systems with attraction. Phys Rev Lett 2008;100:028001.
[31] Viehman DC, Schweizer KS. Cooperative activated dynamics in dense mixtures of hard and sticky spheres. Phys Rev E 2008;78:051404.
[32] Isa L, Besseling R, Weeks ER, Poon WCK. Experimental studies of the flow of concentrated hard sphere suspensions into a constriction. J Phys Conf Ser 2006;40:124–32.
[33] Isa L, Besseling R, Poon WCK. Shear zones and wall slip in the capillary flow of concentrated colloidal suspensions. Phys Rev Lett 2007;98:198305.
[34] Isa L, Besseling R, Morozov AN, Poon WCK. Velocity oscillations in microfluidic flows of concentrated colloidal suspensions. Phys Rev Lett 2009;102:058302.
[35] Besseling R, Isa L, Weeks ER, Poon WCK. Quantitative imaging of colloidal flows. Adv Colloid Interface Sci 2009;146:1–17.
[36] Vermant J, Solomon MJ. Flow-induced structure in colloidal suspensions. J Phys Condens Matter 2005;17:R187–216.
[37] Li Q, Lewis JA. Nanoparticle inks for directed assembly of three-dimensional periodic structures. Adv Mater 2003;15:1639–43.
[38] Prasad V, Semwogerere D, Weeks ER. Confocal microscopy of colloids. J Phys Condens Matter 2007;19:113102.
[39] Weeks ER, Crocker JC, Levitt AC, Schofield AB, Weitz DA. Three-dimensional direct imaging of structural relaxation near the colloidal glass transition. Science 2000;287:627–31.
[40] Dibble CJ, Kogan M, Solomon MJ. Structure and dynamics of colloidal depletion gels: coincidence of transitions and heterogeneity. Phys Rev E 2006;74:041403.
[41] Dibble CJ, Kogan M, Solomon MJ. Structural origins of dynamical heterogeneity in colloidal gels. Phys Rev E 2008;77:050401(R).
[42] Crocker JC, Grier DG. Methods of digital video microscopy for colloidal studies. J Colloid Interface Sci 1996;179:298–310.
[43] Conrad JC, Lewis JA. Structural evolution of colloidal gels during constricted microchannel flow. Langmuir 2010;26:6102–7.
[44] Frank M, Anderson D, Weeks ER, Morris JF. Particle migration in pressure-driven flow of a Brownian suspension. J Fluid Mech 2003;493:363–78.
[45] Semwogerere D, Morris JF, Weeks ER. Development of particle migration in pressure-driven flow of a Brownian suspension. J Fluid Mech 2007;581:437–51.
[46] Conrad JC, Lewis JA. Structure of colloidal gels during microchannel flow. Langmuir 2008;24:7628–34.
[47] Kogan M, Solomon MJ. Electric-field-induced yielding of colloidal gels in microfluidic capillaries. Langmuir 2010;26:1207–13.
[48] Haw M. Jamming, two-fluid behavior, and "self-filtration" in concentrated particulate suspensions. Phys Rev Lett 2004;92:185506.

• Of special interest.
•• Of outstanding interest.

[49] Leighton D, Acrivos A. The shear-induced migration of particles in concentrated suspensions. J Fluid Mech 1987;181:415–39.
[50] Schenker I, Filser FT, Gauckler LJ, Aste T, Herrmann HJ. Quantification of the heterogeneity of particle packings. Phys Rev E 2009;80:021302.
[51] Stickland AD, Buscall R. Whither compressional rheology? J Non-Newtonian Fluid Mech 2009;157:151–7.
[52] Becker EW, Ehrfeld W, Hagmann P, Maner A, Münchmeyer D. Fabrication of microstructures with high aspect ratios and great structural heights by synchrotron radiation lithography, galvanoforming and plastic moulding (LIGA process). Microelectron Eng 1986;4:35–56.
[53] Hruby J. LIGA technologies and applications. MRS Bull 2001;26:337–40.
[54] Liu ZY, Loh NH, Tor SB, Khor KA, Murakoshi Y, Maeda R, et al. Micro-powder injection molding. J Mater Process Tech 2002;127:165–8.
[55] Campbell CJ, Smoukov SK, Bishop KJM, Baker E, Grzybowski BA. Direct printing of 3D and curvilinear micrometer-sized architectures into solid substrates with sub-micrometer resolution. Adv Mater 2006;18:2004–8.
[56] Provin C, Monneret S, Le Gall H, Corbel S. Three-dimensional ceramic microcomponents made using microstereolithography. Adv Mater 2003;15:994–7.
[57] Conrad PG, Nishimura PT, Aherne D, Schwartz BJ, Wu D, Fang N, et al. Functional molecularly imprinted polymer microstructures fabricated using microstereolithography. Adv Mater 2003;15:1541–4.
[58] Benavides GL, Bieg LF, Saavedra MP, Bryce EA. High aspect ratio meso-scale parts enabled by wire micro-EDM. Microsyst Technol 2002;8:395–401.
[59•] Umbanhowar PB, Prasad V, Weitz DA. Monodisperse emulsion generation via drop break off in a coflowing stream. Langmuir 2000;16:347–51.
[60••] Thorsen T, Roberts RW, Arnold FH, Quake SR. Dynamic pattern formation in a vesicle-generating microfluidic device. Phys Rev Lett 2001;86:4163–6.
[61] Anna SL, Bontoux N, Stone HA. Formation of dispersions using "flow focusing" in microchannels. Appl Phys Lett 2003;82:364–6.
[62] Song H, Tice JD, Ismagilov RF. A microfluidic system for controlling reaction networks in time. Angew Chem Int Ed 2003;72:767–72.
[63] Link DR, Anna SL, Weitz DA, Stone HA. Geometrically mediated breakup of drops in microfluidic devices. Phys Rev Lett 2004;92:054503.
[64] Jeong WJ, Kim JY, Choo J, Lee EK, Han CS, Beebe DJ, et al. Continuous fabrication of biocatalyst immobilized microparticles using photopolymerization and immiscible liquids in microfluidic systems. Langmuir 2005;21:3738–41.
[65] De Geest BG, Urbanski JP, Thorsen T, Demeester J, De Smedt SC. Synthesis of monodisperse biodegradable microgels in microfluidic devices. Langmuir 2005;21:10275–9.
[66] Dendukuri D, Tsoi K, Hatton TA, Doyle PS. Controlled synthesis of nonspherical microparticles using microfluidics. Langmuir 2005;21:2113–6.
[67] Xu S, Nie Z, Seo M, Lewis P, Kumacheva E, Stone HA, et al. Generation of monodisperse particles by using microfluidics: control over size, shape, and composition. Angew Chem Int Ed 2005;44:724–8.
[68] Seo M, Nie Z, Xu S, Lewis PC, Kumacheva E. Microfluidics: from dynamic lattices to periodic arrays of polymer disks. Langmuir 2005;21:4773–5.
[69] Seo M, Nie Z, Xu S, Mok M, Lewis PC, Graham R, et al. Continuous microfluidic reactors for polymer particles. Langmuir 2005;21:11614–22.
[70] Nisisako T, Torii T, Higuchi T. Novel microreactors for functional polymer beads. Chem Eng J 2004;101:23–9.
[71] Roh K-H, Martin DC, Lahann J. Biphasic Janus particles with nanoscale anisotropy. Nat Mater 2005;4:759–63.
[72] Dendukuri D, Pregibon DC, Collins J, Hatton TA, Doyle PS. Continuous-flow lithography for high-throughput microparticle synthesis. Nat Mater 2006;5:365–9.
[73] Nie Z, Li W, Seo M, Xu S, Kumacheva E. Janus and ternary particles generated by microfluidic synthesis: Design, synthesis, and self-assembly. J Am Chem Soc 2006;128:9408–12.
[74••] Dendukuri D, Gu SS, Pregibon DC, Hatton TA, Doyle PS. Stop-flow lithography in a microfluidic device. Lab Chip 2007;7:818–28.
[75••] Love JC, Wolfe DB, Jacobs HO, Whitesides GM. Microscope projection photolithography for rapid prototyping of masters with micron-scale features for use in soft lithography. Langmuir 2001;17:6005–12.
[76] Pregibon DC, Toner M, Doyle PS. Multifunctional encoded particles for high-throughput biomolecule analysis. Science 2007;315:1393–6.
[77] Dendukuri D, Hatton TA, Doyle PS. Synthesis and self-assembly of amphiphilic polymeric microparticles. Langmuir 2007;23:4669–74.
[78] Bong KW, Pregibon DC, Doyle PS. Lock release lithography for 3D and composite microparticles. Lab Chip 2009;9:863–6.
[79] Lewis JA. Direct ink writing of 3D functional materials. Adv Funct Mater 2006;16:2193–204.
[80] Lewis JA, Smay JE, Stuecker J, Cesarano J. Direct ink writing of three-dimensional ceramic structures. J Am Ceram Soc 2006;89:3599–609.
[81] Hosokawa M, Nogi K, Naito M, Yokoyama T. Nanoparticle Technology Handbook. 1 ed. Oxford: Elsevier; 2007.
[82] van Osch THJ, Perelaer J, de Laat AWM, Schubert US. Inkjet printing of narrow conductive tracks on untreated polymeric substrates. Adv Mater 2008;20:343–5.
[83] Yoon J, Baca AJ, Park S-I, Elvikis P, Geddes JB, Li L, et al. Ultrathin silicon solar microcells for semitransparent, mechanically flexible and microconcentrator module designs. Nat Mater 2008;7:907–15.
[84] Ahn J-H, Kim H-S, Lee KJ, Jeon S, Kang SJ, Sun Y, et al. Heterogeneous three-dimensional electronics by use of printed semiconductor nanomaterials. Science 2006;314:1754–7.